Energy Engineering
Tech Science Press

http://doi.org/10.32604/ee.2026.074322

ARTICLE

Two-Stage Optimization Scheduling Model for Flexible Resource Aggregation in High-Share Renewable Energy Power Systems Considering Multi-Type Demand Response

Yongzhi Liu, Qiang Li, Qianpeng Hao*, Yaowen Liu, Wenze Li, Zijun Zhao, Zhenyu Chen, Yuxiang Liu, Jiaxing Ren and Wei Han

Inner Mongolia Electric Power (Group) Co., LTD., Hohhot 010010, China
*Corresponding Author: Qianpeng Hao. Email: haoqianpeng666@163.com

Received: 08 October 2025; Accepted: 09 May 2026; Published: 30 August 2026

ABSTRACT: Aiming at the prominent problems of insufficient coordination of multi-type flexible resources and insufficient utilization of demand response potential in high-proportion renewable energy power systems, this paper proposes a two-stage optimal scheduling model for flexible resource aggregation that integrates price-based and segmented incentive-based demand response. In the first stage, the price-based demand response is adopted to optimize the time distribution of elastic loads with the goal of minimizing the net load fluctuation, so as to smooth the net load curve. In the second stage, based on the optimized net load, the segmented incentive-based demand response market mechanism is combined with electrochemical energy storage, pumped storage and flexibility-transformed thermal power units to construct a scheduling model with the minimum system operation cost as the goal. The quadratic terms in the model are linearized by SOS2 constraints, and the Gurobi solver is used for efficient solution. The results show that the proposed model can reduce the net load variance by 46.5%, reduce the system operation cost by 2.33%, avoid the frequent start-stop of thermal power units, significantly enhance the system flexibility and renewable energy consumption capacity, and provide an effective scheduling solution for the safe and economic operation of new power systems.

KEYWORDS: Flexible resource aggregation; two-stage optimization; price-based demand response; incentive-based demand response; high-share renewable energy

1 Introduction

1.1 Motivation

As China's "dual carbon" goals are vigorously advanced, the construction of a new-type power system has become a major national strategic initiative for ensuring energy security and achieving low-carbon transformation [1]. In 2024, three ministries including the National Development and Reform Commission jointly issued the "Action Plan for Accelerating the Construction of a New-Type Power System (2024–2027)", which systematically clarified the stage objectives and implementation pathways for building the new-type power system [2]. In 2025, the National Energy Administration issued the "Notice on Organizing the First Batch of Pilot Projects for New-Type Power System Construction", focusing on seven key directions including grid-forming energy storage, virtual power plants, smart microgrids, and system-friendly new energy power stations. The 2026 "Government Work Report" further listed "making efforts to build a new-type power system and accelerate smart grid construction" as a key annual task. Against this backdrop,

Copyright © 2026 The Authors. Published by Tech Science Press. This work is licensed under a Creative Commons Attribution 4.0 International License, which permits unrestricted use, distribution, and reproduction in any medium, provided the original work is properly cited.

State Grid, China Southern Power Grid, and local grid companies have all increased their investment and deployment, with the total planned grid investment during the "15th Five-Year Plan" period expected to exceed 5 trillion CNY.

From the perspective of supply-side operational characteristics, China's new energy installed capacity maintains rapid growth. By the end of 2025, the total installed capacity of renewable energy reached 2.34 billion kilowatts, a year-on-year increase of 24%, accounting for nearly 60% of the nation's total power installed capacity [3,4]. While large-scale new energy grid integration drives the transformation of the energy structure, it also brings prominent pressure regarding accommodation and regulation. According to statistics from the National New Energy Accommodation Monitoring and Early Warning Center, the national wind curtailment rate in the first half of 2025 was 6.6% and the photovoltaic curtailment rate was 5.7%, with some western provinces rich in new energy resources even experiencing curtailment rates exceeding 30%. Practice has shown that relying solely on traditional thermal power peak shaving and single-type flexible resources has become insufficient to match the multi-time-scale power fluctuations and supply-demand balance requirements under high-proportion new energy access.

From the perspective of flexible resource endowment, China's types of regulation resources are becoming increasingly diverse. By the end of 2025, the national installed capacity of pumped hydro storage reached 65.94 million kilowatts, and the cumulative installed capacity of new-type energy storage exceeded 130 million kilowatts. However, various resources show significant differences in regulation rate, response depth, and economic cost: pumped hydro storage has large regulation capacity but relatively slow response speed and site constraints; electrochemical energy storage responds rapidly but has limited duration; demand-side resources have huge potential but small individual capacity and weak controllability. More critically, these resources are distributed across generation, grid, load, and storage sides, and an efficient collaborative aggregation mechanism and multi-time-scale joint dispatching system have not yet been formed. Common problems include poor coordination between day-ahead planning and intra-day real-time operation, low overall resource utilization, and insufficient release of system regulation potential [5].

In summary, flexible resources are the core guarantee for supporting the safe, stable, and economically efficient operation of high-proportion new energy power systems, and in-depth research is urgently needed.

1.2 Literature Review

Currently, many scholars have conducted extensive research on the operation and dispatch of new-type power systems by aggregating multiple types of flexible regulation resources.

From the perspective of aggregation methods, existing studies focus on quantifying the response capability of demand-side resources and realizing the selection and aggregated regulation of optimal resources through game theory, evaluation models and other approaches. Lu et al. pointed out that resource aggregators (RAs), as emerging market participants, play a crucial role in improving system flexibility, fully tapping the potential of flexible resources, and bridging the gap between demand response (DR) suppliers and purchasers [6]. Zhong et al. proposed a supply-demand side resource aggregation framework, which mobilizes the flexibility of resources by integrating both supply and demand sides and constructs a supply-demand flexibility aggregator [7]. Li et al. used a multi-dimensional index system to quantitatively classify the flexibility of resources, evaluating the power regulation range, energy transfer capacity and dynamic response speed of each resource [8]. Zhu et al. realized resource complementarity through integrating and coordinating various types of distributed energy resources (DERs) via multi-virtual power plants (VPPs), which participate in the market in the form of collaborative clusters, thereby enhancing the power grid regulation capacity and supporting the safe operation of the power system [9]. Zhao et al. proposed a two-layer Stackelberg game model and pointed out that energy storage systems (ES) are crucial for improving the profitability and operational flexibility of VPPs [10]. Liu et al. emphasized that VPPs can provide system flexibility by integrating various DERs and create profit opportunities for DERs simultaneously [11].

In terms of operation and dispatch, existing studies mainly focus on multi-type flexible resources. Jiang et al. studied various types of flexible resources, the supply and demand status of system flexibility, and the optimization of flexible resource scheduling [12]. Pan et al. proposed an optimal scheduling model for integrated energy systems (IES) with flexible supply-demand balance constraints, which significantly improved the flexibility and economy of system operation while reducing the wind curtailment rate [13]. Yang et al. proposed a two-stage operational reliability assessment method for distribution networks considering dynamic scheduling of flexible resources to improve the anti-interference ability of distribution networks and evaluate their operational risks [14]. Zhong et al. proposed a general framework for quantitative evaluation and optimal scheduling of flexible resources to address the problem that the flexibility of different resources has not been fully quantified, supporting the evaluation and scheduling of flexible resources in building district energy systems [15]. Zhang et al. proposed a two-stage scheduling model for flexible resources in active distribution networks (ADN) based on probabilistic risk perception, aiming at the increasing uncertainty of low-carbon power generation energy in ADNs and the difficulty in ADN safety assessment [16]. Hu et al. constructed an IES model that combines the coordination and complementarity of different energy types, the flexible regulation capacity of flexible loads, and the charging and discharging characteristics of ES, thereby improving the matching degree of supply and demand and maximizing the absorption capacity of renewable energy [17]. Mirzaei et al. studied the comprehensive technical, economic and environmental aspects of power distribution and regional heating systems by considering various types of flexible energy resources as well as the environmental and practical limitations of the two networks [18].

To systematically summarize and compare the existing research, Table 1 sorts out the core characteristics, application scenarios and existing gaps of the above representative studies, so as to clearly highlight the research focus of this paper and the differences from previous studies.

In summary, substantial experience has been accumulated in the field of multi-type flexible resource aggregation research. However, there are still obvious limitations in the current literature, which can be specifically summarized as follows:

(1) Most existing studies focus on single-type or partial flexible resources, and lack effective coordination and aggregation of multi-type flexible resources (such as DR, pumped storage, energy storage, and transformed thermal power) as a whole. As shown in Table 1, studies [6,11] only involve single DR or VPP + DER resources, and even studies [7,17] that consider supply-demand side resources do not realize the comprehensive integration of multiple types of flexible resources, resulting in the failure to fully release the system flexibility potential.
(2) The integration of demand response types is not comprehensive, and the combination and sequential application of price-based demand response (PBDR) and incentive-based demand response (IBDR) are rarely considered. From the perspective of DR types in Table 1, most studies only adopt a single IBDR or PBDR, and few studies realize the organic combination of the two; even if studies [7,15] consider both, they do not design a reasonable sequential application mechanism, which cannot give full play to the complementary advantages of different DR types.
(3) Few studies combine the two-stage scheduling framework with the market mechanism, and the existing two-stage scheduling models (such as [14,16]) mainly focus on reliability assessment or risk control,

ignoring the guidance role of the market mechanism in resource aggregation and scheduling, which leads to difficulty in balancing the safety and economy of system operation.

(4) The existing resource aggregation and scheduling models lack detailed modeling of the characteristics of various flexible resources, and cannot fully adapt to the differences in response speed, regulation depth and cost characteristics of different resources, resulting in insufficient optimization effect of the scheduling scheme.

Table 1: A comparative sumumary of this study and previous publications.

Ref	Aggregation Approach	DR Type	Resources	Two-Stage	Market Mechanism	Problem Type	Key Gap
[6]	Resource aggregator	IBDR	DR only	×	✓	Optimization	No multi-resource coordination
[7]	Game theory	PBDR + IBDR	Supply + demand	×	✓	Multi-objective + Game	No detailed resource modeling
[8]	Hierarchical MPC	PBDR	Park IES	×	✓	MPC	Single time-scale
[9]	Multi-agent game	IBDR	Multi-VPP	×	✓	Stackelberg game	No PBDR-IBDR sequence
[10]	Bilevel optimization	IBDR	VPP + ES	×	✓	Bilevel	ES pricing only
[11]	Distribution market	IBDR	VPP + DER	×	✓	Optimization	No PBDR
[12]	Integrated planning	–	WT + PV + TP + PS	×	×	Optimization	No DR, no market
[13]	Q-learning + GWO	–	IES + H2	×	×	Heuristic	No optimality guarantee
[14]	Two-stage reliability	IBDR	Flexible resources	✓	×	Two-stage	Reliability focus, no economic opt.
[15]	Quantitative assessment	PBDR + IBDR	Building district	×	×	Assessment	No scheduling opt.
[16]	Probabilistic risk	IBDR	ADN resources	✓	×	Two-stage stochastic	Risk-based, no market
[17]	IES modeling	–	Supply + demand + ES	×	×	Optimization	No DR, no two-stage
[18]	Multi-energy network coordination	–	Flexible energy resources	×	×	Multi-objective assessment	No DR integration
This study	Two-stage aggregation	PBDR + Segmented IBDR	WT + PV + TP + ES + PS + DR	✓	✓	MILP	–

1.3 Our Contributions

To address the above research gaps, this paper introduces innovative research in three main aspects:

(1) A two-stage flexible resource aggregation framework with progressive coupling. Unlike existing studies that optimize demand response and unit dispatch separately, this paper establishes a two-stage model

with clear progressive coupling: the first-stage PBDR output serves as the input for the second-stage IBDR and unit dispatch optimization. This ensures temporal consistency between load curve shaping and real-time resource scheduling.

(2) Comprehensive integration of multi-type demand response mechanisms. This paper simultaneously incorporates price-based demand response (PBDR) and segmented incentive-based demand response (IBDR), designing a sequential application mechanism that leverages PBDR for load curve smoothing and IBDR for peak load curtailment and upward reserve provision. This overcomes the limitation of existing studies that only utilize single-type DR.

(3) Detailed modeling of flexibility-retrofitted thermal power characteristics. The model captures the operational characteristics of flexibility-retrofitted thermal power units, including reduced minimum technical output, increased ramp rates, and shortened start-stop times. This enables quantitative evaluation of the marginal contribution of thermal power flexibility upgrades to system operation costs and start-stop performance.

1.4 Organization of This Paper

The remainder of this paper is organized as follows. Section 2 analyzes the operating characteristics of flexible resources in the new power system. Section 3 constructs a two-stage optimization scheduling model for flexible resource aggregation: the first stage optimizes the price-based demand response to minimize net load fluctuation, and the second stage coordinates segmented incentive-based demand response with multi-type flexible resources to minimize system operating costs. Section 4 presents the model solution methodology, where the quadratic programming problem is linearized using Special Ordered Sets of Type 2 (SOS2) constraints and solved by the Gurobi solver. Section 5 conducts case studies based on a regional power system, analyzing the optimization results and comparing four scenarios to verify the effectiveness of the proposed model. Section 6 concludes the paper and outlines future research directions.

2 Modeling of Flexible Resource Operating Characteristics

In the process of building a new type of power system, the aggregation and coordinated operation of flexible resources have become the core link for enhancing the resilience and regulation capabilities of the system [19]. The specific operational structure is shown in Fig. 1.

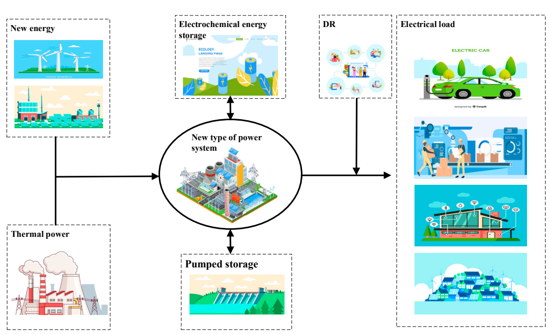

Figure 1: System operation structure diagram.

As shown in Fig. 1, this aggregation system takes new energy sources such as wind power and photovoltaic power as the main power sources, deeply integrating flexible and energy-saving retrofitted thermal power units, energy storage equipment, and pumped storage power generation and other types of flexible regulation resources. It forms a dynamic operation architecture of “source-network-load-storage” interaction. Among them, the retrofitted thermal power units mainly undertake basic regulation and backup support. Energy storage and pumped storage achieve power balance and energy time shift within seconds to hours, while the demand response mechanism drives traditional rigid loads to gradually transform into flexible adjustable loads, enabling end users to actively participate in system peak shaving and valley filling. In addition, the operation system achieves coordinated control at different levels and zones and market signal guidance. Each flexibility regulation resource optimally complements each other on the day-ahead, intraday, and real-time time scales, jointly ensuring the safe, stable, and economically efficient operation of the new power system with a high proportion of new energy.

The basic models for the operational characteristics of each unit participating in the new power system are as follows:

(1) Flexible-modified thermal power generating units

The flexibility transformation of thermal power plants is an important technical approach for deep adaptability upgrades of existing thermal power units. Its core objective is to enhance the unit's peak regulation and response capabilities in the new power system, thereby better matching the fluctuating and intermittent output characteristics brought about by the large-scale integration of new energy. After the flexibility transformation, thermal power units mainly optimize three aspects of operational performance: first, reducing the minimum technical output of the unit; second, increasing the power ramp rate; and third, shortening the unit's start-up and shutdown time [20]. Although the flexibility transformation involves the operation adjustments and parameter optimizations of multiple subsystems within the plant, such as boilers, steam turbines, and auxiliary equipment, it does not change the basic working principle and energy conversion mechanism of the thermal power unit. The coal consumption characteristics of the unit still follow the quadratic function rule related to power, as shown in the following equation.

$$C_{TP,u,t}^{coal} = a_i(P_{TP,i,t})^2 + b_iP_{TP,i,t} + c_i \tag{1}$$

where, $C_{TP,u,t}^{coal}$ represents the coal consumption of Thermal Power (TP) unit i at time t; a_i, b_i, c_i are the coal consumption parameters; $P_{TP,i,t}$ is the output power of TP unit i at time t.

(2) New energy generating units

2.1 PV Model

The power output of photovoltaic power generation is mainly influenced by the intensity of light. Its output characteristics are closely related to the solar irradiance. The specific mathematical model is as follows.

$$P_{pv,t} = \eta_{pv}S_{pv}\theta_t \tag{2}$$

where, $P_{pv,t}$ represents the power output of the photovoltaic (PV) system at time t; η_{pv} is the efficiency of the PV system; S_{pv} is the area of the PV panels; θ_t represents the solar irradiance at time t.

2.2 WT Model

The output power of the wind turbine is directly determined by the actual wind speed acting on the hub of the turbine. However, in actual engineering and meteorological observations, the wind speed data is often not collected at the hub height. Therefore, a wind speed-height conversion relationship is needed to convert the measured wind speed to the hub height in order to accurately calculate the wind power. The specific basic model is as follows.

$$P_{wt,t} = \begin{cases} 0, v_{h,t} < v_{in} or v_{h,t} \geq v_{out} \\ \eta_{wt} P_{wt}^{\max} \frac{v_{h,t} - v_{in}}{v_r - v_{in}}, v_{in} \leq v_{h,t} \leq v_r \\ \eta_{wt} P_{wt}^{\max}, v_r \leq v_{h,t} \leq v_r \end{cases} \tag{3}$$

where, $P_{wt,t}$ represents the power output of the wind turbine (WT) at time t; η_{wt} is the efficiency of the wind turbine; $P_{wt}^{\max}$ is the rated power; v_{in}, v_r, v_{out} represents the cut-in, rated, and cut-out wind speeds, respectively.

2.3 ES Model

The energy storage system (ES) charges by absorbing electrical energy during periods of low electricity demand, and discharges the stored energy during peak demand periods to meet the power supply requirements. This enables the transfer and optimal allocation of electrical energy over time. In the new power system operation system, energy storage can effectively smooth out load fluctuations, play the typical role of peak shaving and valley filling, and enhance the operational stability and economy of the system. The specific basic model is as follows.

$$C_{ES,t} = C_{ES,t-1} + \eta_{ES} P_{ES,t}^{chr} - \frac{1}{\eta_{ES}} P_{ES,t}^{dis} \tag{4}$$

where, $C_{ES,t}$ represents the stored energy of the Energy Storage (ES) system at time t; η_{ES} is the efficiency of the ES system; $P_{ES,t}^{chr}, P_{ES,t}^{dis}$ represents the charging and discharging power, respectively.

2.4 PS Model

The pumped storage unit (PS) is equipped with two reservoirs, forming a complete energy storage and release system. During periods when the electricity load in the power system is low, the unit utilizes the excess electricity to pump water from the lower reservoir to the upper reservoir to complete energy storage; during peak electricity load periods, water is released from the upper reservoir to drive the unit to generate electricity. This operation mode enables the transfer and redistribution of electrical energy on a time scale, and in the new power system, it plays an important role in peak shaving and valley filling regulation functions. The specific basic model is as follows.

$$V_{PS,t}^{up} = V_{PS,t-1}^{up} - \sum_{j=1}^{J} Q_{PS,j,t}^{gene} + \sum_{j=1}^{J} Q_{PS,j,t}^{pump} \tag{5}$$

$$V_{PS,t}^{down} = V_{PS,t-1}^{down} + \sum_{j=1}^{J} Q_{PS,j,t}^{gene} - \sum_{j=1}^{J} Q_{PS,j,t}^{pump} \tag{6}$$

where, $V_{PS,t}^{up}$ represents the water storage volume in the upper reservoir of the Pumped Storage (PS) system at time t; J is the number of PS units; $Q_{PS,j,t}^{gene}$ is the water consumption for electricity generation by the j-th PS unit at time t; $Q_{PS,j,t}^{pump}$ is the water pumping volume by the j-th PS unit at time t.

3 Construct a Two-Stage Scheduling Optimization Model

3.1 Problem Description

Based on the multi-type flexibility resources' participation in the operation and dispatch of the new power system as discussed in Section 2, this section further studies how to coordinate the temporal coordination of price-based demand response and incentive-based demand response, so as to reduce the net load fluctuation and achieve the optimal operation cost of the new power system. By constructing a two-stage optimization scheduling model for flexibility resource aggregation, and with a clear progressive coupling relationship between the two stages, the load curve optimized in the first stage serves as the input for the second stage, and the decisions made in the previous stage directly affect the feasible region and objective function of the subsequent stage.

The two main core problems addressed are as follows:

- Problem 1 (First stage: Price-based demand response optimization). How to guide users to adjust their electricity consumption behavior through price signals, taking into account the peak-valley difference of the load and the output power of wind and solar power, to optimize the spatio-temporal distribution of the elastic load, in order to reduce the fluctuation of the net load curve.
- Problem 2 (Second stage: Incentive-based demand response and resource scheduling optimization). Based on the net load optimized in the first stage, how to encourage users to declare interruptible loads through incentive signals and coordinate the scheduling of flexibility resources such as thermal power and energy storage, with the goal of minimizing the system operation cost, to obtain the optimal scheduling plan.

3.2 Two-Stage Optimization Scheduling Model

3.2.1 Objective Function

This paper aims to enhance the flexibility of the new power system and proposes a two-stage scheduling optimization model for flexibility resource aggregation.

(1) The first stage of optimizing the model

The first-stage model (F_{upper}) takes into account time-varying price-based demand response, aiming to smooth the load curve by minimizing the net load fluctuation. The details are as follows.

$$\min F_{upper} = \sum_{t=1}^{T}\left(L_t - P_{wt,t}^{fore} - P_{pv,t}^{fore} - \frac{1}{T}\sum_{t=1}^{T}(L_t - P_{wt,t}^{fore} - P_{pv,t}^{fore})\right)^2 \tag{7}$$

where, L_t represents the load after the implementation of the price-based demand response mechanism; $P_{wt,t}^{fore}$, $P_{pv,t}^{fore}$ represents the predicted power for wind power and photovoltaic power, respectively.

(2) The second stage of optimizing the model

The second-stage model (F_{lower}) considers the segmented incentive-based demand response market trading mechanism, integrating electrochemical energy storage, pumped storage, and the renovation of thermal power plants, and designs the optimal operation plan by minimizing the system operation cost. The details are as follows [21].

$$\min F_{lower} = \sum_{t=1}^{T} \sum_{i=1}^{n} \left((\tau_{coal} F_{TP,i,t} + u_{i,t}^{up} \tau_{coal} F_{TP,i}^{up} + u_{i,t}^{down} \tau_{coal} F_{TP,i}^{down}) + (\pi_R^{up} R_t^{up} + \pi_R^{down} R_t^{down}) + C_t^{cur} \right) \quad (8)$$

where, τ_{coal} represents the price of coal; $u_{i,t}^{up}$, $u_{i,t}^{down}$ represents the coal consumption for the startup and shutdown of flexible-modified thermal power units; $F_{TP,i}^{up}$, $F_{TP,i}^{down}$ represents binary variables, indicating the flexibility transformation of the start and stop operations of thermal power generating units. 0 indicates no action, while 1 indicates action. The values of π_R^{up} and π_R^{down} in decibels represent the system's overhead cost coefficients; R_t^{up}, R_t^{down} represents the backup requirements for the system at the upper and lower levels, respectively; C_t^{cur} represents the total compensation cost of IBDR.

3.2.2 Constraint Conditions

The optimization process in the first stage satisfies the following constraints.

(1) Load variation quantity

As the peak-valley load difference of the power grid continues to widen, price-based demand response (PBDR), as a user-side regulation method based on time-of-use electricity price signals, has been widely applied to guide users to adjust their electricity consumption behaviors, thereby achieving the optimization and smoothing of the load curve. When $s = t, e_{st} \leq 0$ indicates that an increase in the electricity price during a certain period will lead to a decrease in the electricity load during that period, it reflects the "self-price elasticity" of users. When $s \neq t, e_{st} > 0$ represents that changes in electricity prices during other periods will trigger reverse adjustments in the electricity load of this period, it reflects the "cross-price elasticity" of users, that is, the behavior where users shift their loads to periods with lower electricity prices. Its core mechanism is quantitatively characterized by the demand price elasticity coefficient matrix, which is defined as follows:

$$e_{st} = \frac{\Delta L_s / L_s^0}{\Delta P_t / P_t^0} \begin{cases} e_{st} \leq 0, s = t \\ e_{st} > 0, s \neq t \end{cases} \quad (9)$$

where, ΔL_s represents the load variation in period s after implementing demand response; L_s^0 represents the baseline load for period s before the implementation of demand response; ΔP_t represents the change in electricity price during period t after the implementation of time-of-use pricing; P_t^0 represents the base price for period t before the implementation of time-of-use electricity pricing.

(2) Periodic load total quantity conservation constraint

To ensure that the load energy remains balanced on an overall scale before and after the implementation of demand response, strict constraints need to be imposed on the cumulative load in each typical period (peak, valley, and flat):

1. The sum of the loads at all times during the peak period is equal to the total load for that period, as follows:

$$\sum_{t \in peak} L_t = L_p \quad (10)$$

2. The sum of the loads at all times during the valley period is equal to the total load for that period. As follows:

$$\sum_{t \in valley} L_t = L_p \tag{11}$$

3. The sum of the loads at all times during the regular period is equal to the total load for that period. As follows:

$$\sum_{t \in regular} L_t = L_p \tag{12}$$

The aforementioned relationship ensures that the total electricity consumption remains structurally unchanged across all time periods, merely facilitating the migration and reorganization of the load over the time axis.

(3) Load response amplitude limit conditions

Due to the rigid nature of some loads and the fact that user participation is constrained by factors such as electricity satisfaction, the load adjustment capacity is not unlimited. Therefore, a reasonable response boundary needs to be set. The details are as follows:

$$L_t^0(1-\sigma) \le L_t \le L_t^0(1+\sigma) \tag{13}$$

where, L_t^0 represents the baseline load when PBDR is not involved; σ represents the maximum achievable response level for the user. This parameter limits the range of load shift, preventing excessive response from causing unstable power supply or a decline in user experience.

(4) Power purchase cost optimization constraint

The core driving force for motivating users to participate in demand response is the reduction of their overall electricity purchase cost, as shown in the following formula.

$$\sum_{t=1}^{T} \sigma_t L_t \le \sum_{t=1}^{T} \sigma_t^0 L_t^0 \tag{14}$$

where, σ_t represents the time-of-use electricity price after implementing demand response; σ_t^0 represents the base electricity price. This constraint ensures that the total electricity cost on the user side does not increase after the response behavior, thereby achieving consistency between the user's participation intention and the system optimization goal.

- The optimization process in the second stage satisfies the following constraints.

1. Global power balance constraint

The system must satisfy the net power supply-demand balance at each moment. That is, the total output of wind power, photovoltaic power, thermal power, energy storage and pumped storage power should be consistent with the net load after deducting the demand response reduction amount from the load, as shown in the following equation:

$$P_{wt,t} + P_{pv,t} + \sum_{i}^{n} P_{TP,i,t}(1-\eta_{TP,i}) + (P_{ES,t}^{dis} - P_{ES,t}^{chr}) + \sum_{j=1}^{J} (P_{PS,j,t}^{gene} - P_{PS,j,t}^{pump}) = L_t - L_t^{cur} \tag{15}$$

where, $\eta_{TP,i}$ represents the auxiliary power consumption rate of the TP plant; L_t^{cur} represents the load reduction amount after demand response.

2. Output constraints of renewable energy sources

The power output of wind power and photovoltaic power is restricted by natural conditions and both need to satisfy the non-negativity and rated capacity boundaries, as shown in the following equation:

Wind power output constraint:

$$0 \le P_{wt,t} \le P_{wt,t}^{\max} \tag{16}$$

Photovoltaic output constraint:

$$0 \le P_{pv,t} \le P_{pv,t}^{\max} \tag{17}$$

The aforementioned constraints ensure that the output of renewable energy remains within the physically feasible range.

3. Flexible modification of operating constraints for thermal power plants

After undergoing flexibility upgrades, thermal power units perform better than traditional units in terms of output range, regulation rate, and start-stop characteristics, as shown in the following formula.

Output range constraint:

$$u_{i,t}P_{TP,i}^{\min} \le P_{TP,i,t} \le u_{i,t}P_{TP,i}^{\max} \tag{18}$$

where, $u_{i,t}$ is the binary variable representing the start-up and shut-down status of thermal power.

Slope climbing rate constraint:

$$-P_{TP,i}^{down} \le P_{TP,i,t} - P_{TP,i,t-1} \le P_{TP,i}^{up} \tag{19}$$

where, $P_{TP,i}^{down}$ and $P_{TP,i}^{up}$ represent the downward and upward ramp rate limits, respectively.

Activate logical constraints:

$$u_{i,t} - u_{i,t-1} - u_{i,t}^{up} \le 0 \tag{20}$$

$$u_{i,t-1} - u_{i,t} - u_{i,t}^{down} \le 0 \tag{21}$$

Minimum start-up/shutdown time constraint:

$$u_{i,t} - u_{i,t-1} - u_{i,k} \le 0, \forall k \in [t, T_i^{on} + t - 1] \tag{22}$$

$$u_{i,t-1} - u_{i,t} + u_{i,k} \le 1, \forall k \in [t, T_i^{off} + t - 1] \tag{23}$$

where, T_i^{on} represents the minimum continuous operating time, and T_i^{off} represents the minimum continuous shut-down time.

4. Electrochemical Energy Storage (ES) operational constraints

Energy storage must satisfy core constraints such as mutually exclusive charging and discharging, power boundaries, and energy conservation. Additionally, to extend the lifespan, the range of available energy needs to be limited, as shown in the following equation:

$$\mu_{ES,t}^{chr/dis} P_{ES}^{chr/dis,\min} \leq P_{ES,t}^{chr/dis} \leq \mu_{ES,t}^{chr/dis} P_{ES}^{chr/dis,\max} \tag{24}$$

where, $\mu_{ES,t}^{chr/dis}$ are the binary state variables for charging and discharging of ES.

5. Pumped Storage (PS) Operation Constraints

$$u_{PS,j,t}^{gene} P_{PS}^{gene,\min} \leq P_{PS,j,t}^{gene} \leq u_{PS,j,t}^{gene} P_{PS}^{gene,\max} \tag{25}$$

$$u_{PS,j,t}^{pump} P_{PS}^{pump,\min} \leq P_{PS,j,t}^{pump} \leq u_{PS,j,t}^{pump} P_{PS}^{pump,\max} \tag{26}$$

$$u_{PS,j,t}^{gene} + u_{PS,j,t}^{pump} \leq 1 \tag{27}$$

where, $u_{PS,j,t}^{gene}, u_{PS,j,t}^{pump}$ are the binary state variables for generating and pumping modes of Pumped Storage (PS), respectively.

6. Incentive-based demand response (IBDR) segmentation constraints

During peak hours, load reduction through the segmented IBDR mechanism can effectively alleviate the peak regulation pressure. By combining segmented quotations with duration requirements, the following constraints are established:

The composition of load reduction amount is as follows:

$$L_t^{cut} = u_t^{cur} L_{t,1}^{cur,\min} + \sum_{m=2}^{M} L_{t,m}^{cur} \tag{28}$$

$$0 \leq L_t^{cur} \leq u_t^{cur} L_{t,M}^{cur,\max} \tag{29}$$

7. System backup capacity constraint

To cope with load variations and fluctuations in new energy sources, it is necessary to ensure the balance of supply and demand for up and down backup capacity, as shown in the following equation:

$$R_{TP,t}^{up} + R_{ES,t}^{up} + R_{PS,t}^{up} + R_{IBDR,t}^{up} \geq R_t^{up} \tag{30}$$

$$R_{TP,t}^{down} + R_{ES,t}^{down} + R_{PS,t}^{down} \geq R_t^{down} \tag{31}$$

where, $R_{TP,t}^{up}, R_{ES,t}^{up}, R_{PS,t}^{up}, R_{IBDR,t}^{up}$ represents the upward reserve capacity provided by various resources, respectively; $R_{TP,t}^{down}, R_{ES,t}^{down}, R_{PS,t}^{down}$ represents the downward reserve capacity provided by various resources, respectively.

4 Model Solution Method

In the two-stage scheduling optimization model for aggregating flexibility resources in the new power system structure developed in this paper, the first-stage price-based demand response optimization problem essentially belongs to a quadratic programming (Quadratic Programming, QP) problem. Considering that the existence of quadratic terms in the scheduling scenarios of large-scale power systems will significantly increase the complexity of model solution, this paper uses the current mainstream commercial solver

(Gurobi) for solving, and introduces special ordered sets of type 2 (Special Ordered Sets of Type 2, SOS2) constraints to linearize the quadratic function terms in the model, converting the problem into an equivalent mixed integer linear programming (Mixed Integer Linear Programming, MILP) form that can be efficiently solved. The specific calculation process is shown in Fig. 2.

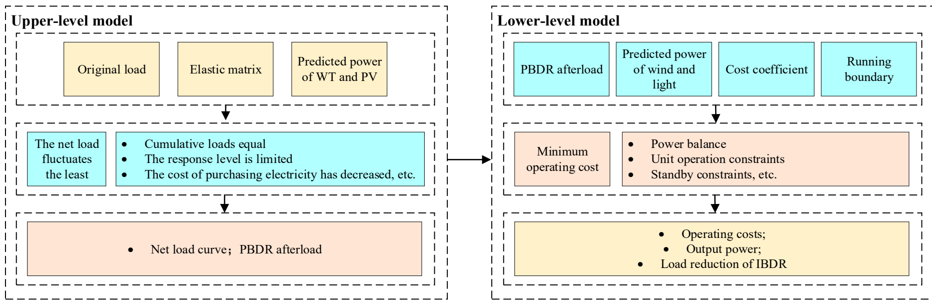

Figure 2: The solution process of the two-stage optimization optimization model.

As shown in Fig. 2, the quadratic function is approximated by a piecewise linear function. By introducing weight variables and binary variables, it is ensured that the function is obtained through linear interpolation between any two adjacent piecewise points at any given time.

5 Case Study Analysis

5.1 Data Information

To verify the improvement effect of the proposed model on the flexibility of the power system, a certain regional power system was selected as the demonstration project for simulation research. This demonstration project system includes various power sources such as wind and solar energy, flexible-reconfiguration thermal power, and energy storage devices, along with a peak-valley time-of-use electricity pricing mechanism and demand response measures. The specific system parameters are shown in Table 2.

Table 2: Basic Information of Power Supply.

Power Type	Installed Capacity/MW
WT	2600
PV	3200
Flexible retrofitted thermal power generation	11,000
Electrochemical energy storage	100 MW/240 MW.h
Pumped storage power station	1000

The daily load curve, wind power prediction curve, and photovoltaic power prediction curve of this demonstration project system are shown in Fig. 3; the corresponding flexible thermal power units total 20, among which the maximum installed capacity is 300 MW, the minimum installed capacity is 40 MW, the average start-stop time is 2.55 h, and the average start-stop coal consumption is 6.9 t per time. The operating parameters of the accompanying electrochemical energy storage system and the equipment parameters of the pumped storage power station are referred to in References [22,23].

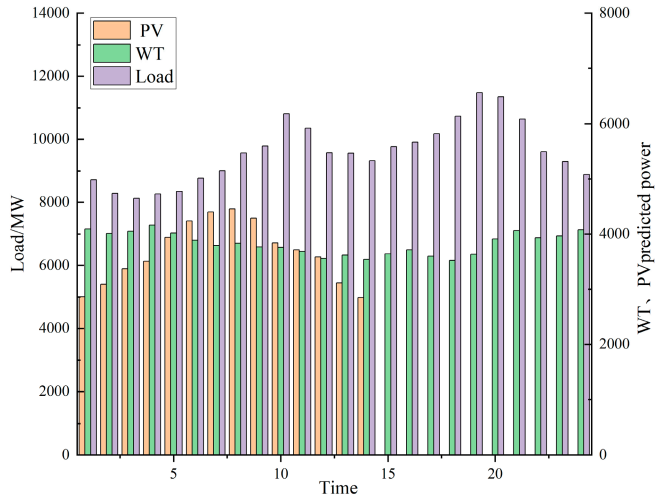

Figure 3: System load and predicted WT and PV.

Meanwhile, this area implements peak-valley time-of-use electricity pricing, with a price difference ratio of 4:1 (as shown in Table 3), and introduces a price-based demand response mechanism (PBDR), with the maximum response rate being 5%. The incentive-based demand response mechanism (IBDR) reduces load based on the time-of-use electricity pricing.

Table 3: Electricity tariff execution situation.

Type	Time Period	Price (CNY/kWh)
Peak period	10:00–11:00, 18:00–21:00	0.2521
Regular period	8:00–9:00; 15:00–17:00; 22:00–24:00	0.6288
Valley period	The remaining periods	1.0078

5.2 Result Analysis and Discussion

Result Analysis

In order to verify the validity and scientificity of the proposed model, the results of the above demonstration project were analyzed as follows:

(1) Analysis of the results of the first-stage optimization

The user load curves obtained after implementing the PBDR mechanism are shown in Figs. 4 and 5.

From Figs. 4 and 5, it can be seen that, on the one hand, after implementing the PBDR mechanism, the overall trend of the net load curve remains largely consistent with that before implementation, but the degree of fluctuation has significantly decreased—the variance of the original net load curve was 3.522×10^8 MW^2, and after optimization by the PBDR mechanism, it dropped to 188.2 million MW^2, a reduction of nearly 50%. On the other hand, compared with the original load structure, the peak load during peak hours has been effectively reduced, with the maximum load decreasing from 11,655 MW to 10,722 MW; while the load during off-peak and normal hours has increased, with the minimum load rising from 8233 MW to 8457 MW. Moreover, the PBDR mechanism makes the load curve more gentle, effectively alleviating the peak-load regulation pressure of the new power system, and at the same time, the purchase cost of users has also decreased by 6.88%.

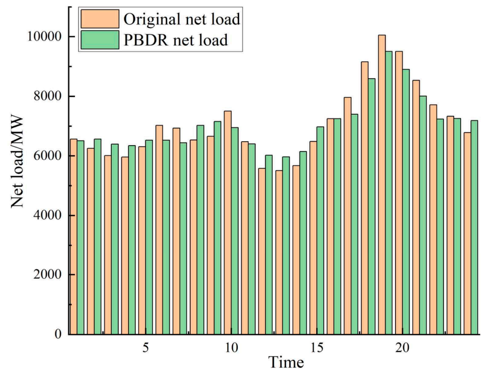

Figure 4: Original net load curve and net load curve after PBDR.

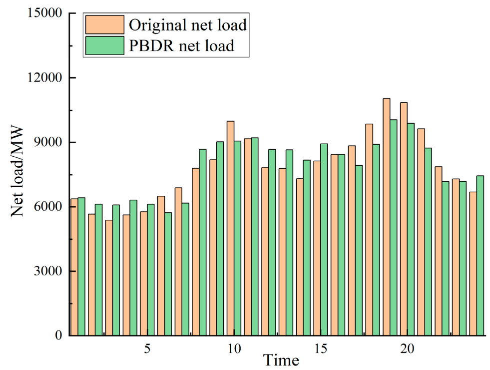

Figure 5: Original load curve and load curve after PBDR.

(2) Analysis of the optimization results in the second stage

By integrating the load curve input from the PBDR implementation in the first-stage model into the second-stage model, and considering segmented IBDR in actual scheduling, various flexibility resources are utilized to meet the system's electricity and power demand. The clearing results and the available upper and lower reserve capacities of various flexibility resources are shown in Figs. 6 and 7.

As can be seen from Figs. 6 and 7, the clearing results of the segmented Incentive-Based Demand Response (IBDR) present a clear time division of labor. The first clearing occurs during 00:00–05:00, and its goal is not to directly curtail the load, but to provide upward reserve capacity for the system—that is, when the load surges or the renewable energy output drops sharply, the IBDR resources are called to quickly reduce electricity consumption, which is equivalent to increasing the upward regulation capacity on the power generation side. This alleviates the reserve pressure of thermal power units, enables thermal power to operate more stably near the rated operating condition, and reduces the opportunity cost caused by frequent output adjustments. The second clearing takes place during 14:00–20:00, a period corresponding to the system's evening peak. During this period, IBDR directly implements load curtailment to reduce peak demand and avoid starting high-cost peaking units. From the perspective of the reserve capacity of various flexible resources (Fig. 8), the overall downward reserve capacity of the system is very sufficient, which can easily cope with scenarios that require output reduction such as load decline or renewable energy over-generation; although the absolute value of the upward reserve capacity is small, it can still meet the reserve margin required for renewable energy fluctuations and random load changes after combining the contributions of pumped storage and IBDR. Specifically, pumped storage provides considerable upward reserve during 06:00–11:00 (morning ramping period) and 18:00–21:00 (before the evening peak), while

IBDR provides upward reserve during 00:00–05:00 (early morning valley) and 13:00–19:00 (afternoon to evening). The two complement each other in time, almost covering the most critical reserve demand windows throughout the day, which significantly reduces the extent to which thermal power is forced to participate in frequent regulation and enables thermal power units to operate in the economic load zone for more time.

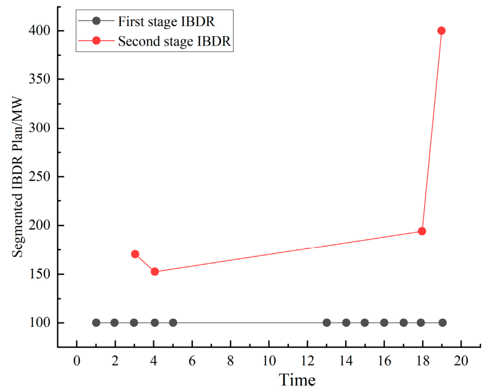

Figure 6: Segmented incentive demand-response plan.

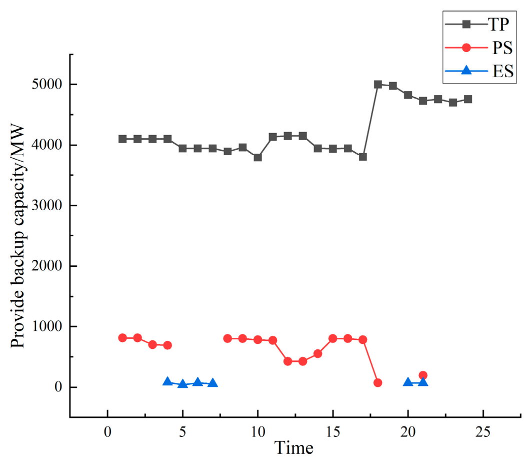

Figure 7: Upper and lower standby capacity available from various flexible resources.

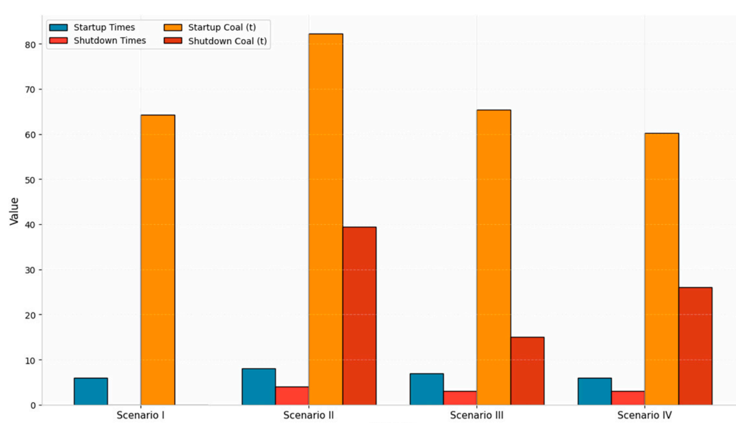

Figure 8: Startup and shutdown times and coal consumption of thermal power in each scenario.

1. The operating status of thermal power units, as shown in Figs. 9 and 10.

As can be seen from Figs. 9 and 10, the output data of the seven thermal power units (TP1~TP7) within 0~24 h show that all units maintained continuous operation without any start-up or shutdown operations. Among them, the outputs of TP1, TP2, TP3, TP5, TP6, and TP7 remained constant throughout the 24 h, being 1000 MW, 600 MW, 400 MW, 250 MW, 200 MW, and 150 MW, respectively. In contrast, the output of TP4 gradually increased from 300 MW at 00:00 to 362 MW at 24:00, with a cumulative increase of 62 MW and a growth rate of 20.7%.

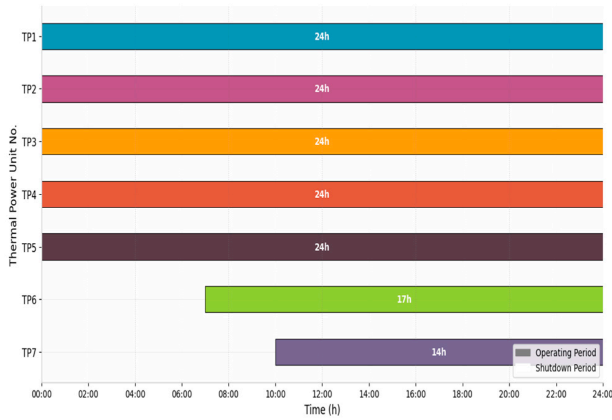

Figure 9: Output power of thermal power units.

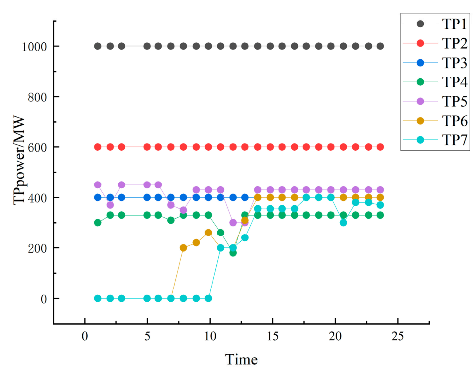

Figure 10: Output power of thermal power units.

- From the perspective of unit operation safety, all units operated without start-up and shutdown throughout the day, avoiding problems such as low-cycle fatigue of steam turbine rotors, thermal stress on boiler heating surfaces, and insulation aging of generators caused by frequent thermal cycles. This significantly extends the service life of equipment and reduces the risk of unplanned outages. The ramping characteristics of TP4 are also very stable, with a maximum hourly output increment of 5 MW. Taking the rated capacity of a typical coal-fired unit of 500 MW as an example, the ramping rate is only 1% rated power per hour, which is much lower than the allowable 2~5% rated power per minute for conventional thermal power units. Such an extremely low ramping rate means that the system has low requirements for load tracking capability, and the unit can operate stably at a certain operating point for a long time, hardly generating additional thermal stress or control difficulties.
- From the perspective of economic dispatch, units with constant output are usually arranged to operate in the minimum coal consumption zone (such as 85%~95% of rated power). Therefore, TP1 (1000 MW),

TP2 (600 MW), and TP3 (400 MW) may be at their respective optimal efficiency points; as small-capacity units, TP5 (250 MW), TP6 (200 MW), and TP7 (150 MW) often have higher heat consumption rates than large units, but they play the role of intermediate load in the system, which can avoid efficiency deterioration caused by deep peak shaving of large units. TP4 increased from 300 MW to 362 MW, always in the medium load range, and its thermal efficiency may be slightly lower than that at full load. However, as the only regulating unit, it undertakes all load climbing tasks, resulting in a large number of load changes and a long time away from the optimal operating condition, and the unit power generation coal consumption may increase by about 1~3 g/kWh.

- From the perspective of fuel cost estimation, the total power generation (calculated at an average hourly output of about 2931 MW, about 70,344 MWh per day) increased by 62 MW, resulting in an additional power generation of about 1488 MWh. If the fuel cost is 0.3 CNY/kWh, the additional fuel cost is about 446 CNY, with a negligible economic impact. However, in the market environment, the additional 62 MW power generation of TP4 can bring marginal benefits to the power plant, especially when the spot electricity price is high, this slow power increase strategy can capture price dividends.
- Importantly, an obvious disadvantage of the dispatch strategy is the excessive reliance on a single unit for regulation. When TP4 needs to further increase its output, its capacity is close to 362 MW. If the system load continues to rise, there will be no regulation margin; on the contrary, if the load decreases, TP4 needs to reduce its output, but other constant units cannot cooperate quickly, which may cause reverse peak shaving or curtailment of wind and solar power.

2. The operation status of the electrochemical energy storage unit is shown in Fig. 11.

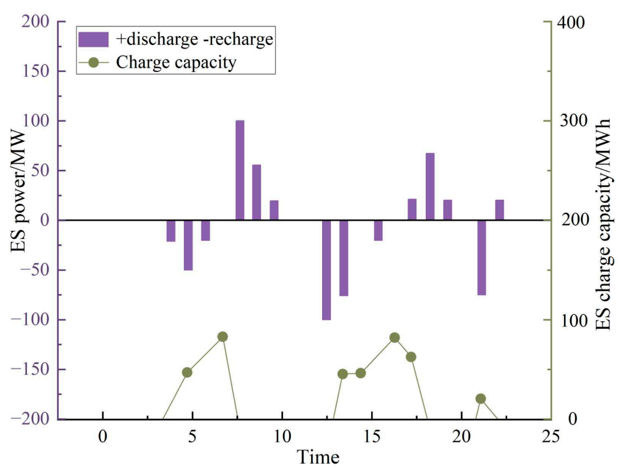

Figure 11: Charge and discharge power and storage capacity of electrochemical energy storage.

As can be seen from Fig. 11, the storage battery experiences 2 full charge states and 1 full discharge state throughout the day: the first full charge occurs at the end of the early morning charging period, and then it is completely discharged during the morning peak discharge process; the second full charge appears at the end of the afternoon charging period, and then it is discharged completely again during the evening peak discharge. Through this “two charges and one discharge” dispatch mode, the energy storage effectively suppresses the net load fluctuation, reduces the curtailment of wind and solar power, significantly alleviates the system peak shaving pressure, and fully exerts the flexible regulation and energy time-shifting functions of electrochemical energy storage.

3. The operating status of the pumped storage power station is shown in Figs. 12 and 13.

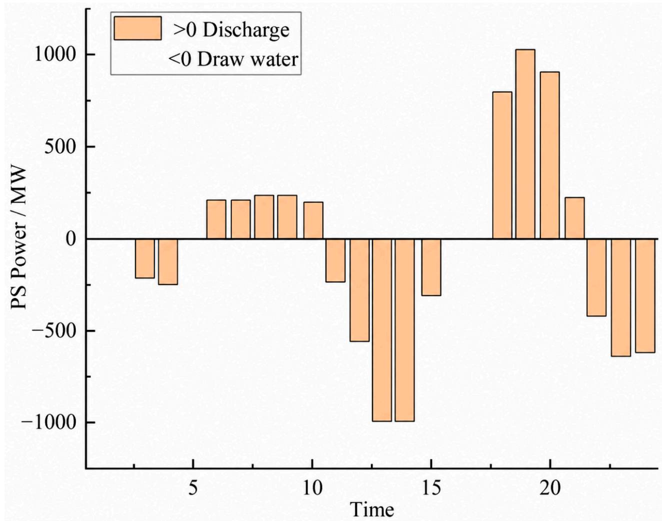

Figure 12: Pump storage power and pumping status.

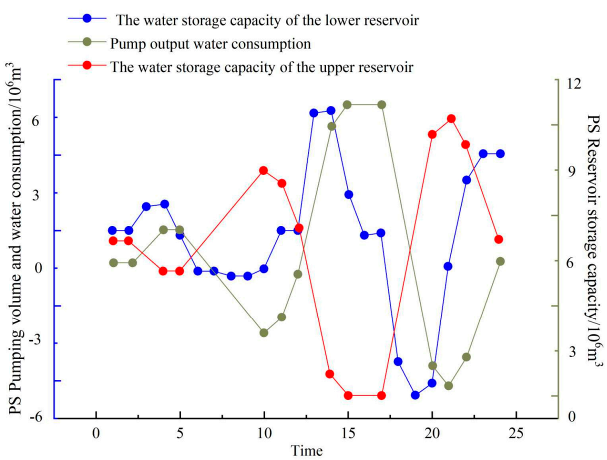

Figure 13: Reservoir water storage dynamics.

As can be seen from Figs. 12 and 13, the charging and discharging process of the pumped storage power station presents a highly coordinated "pumping-power generation" cycle with the changes in reservoir water volume. It can be seen from the power curve (Fig. 12) that the pumped storage power station mainly operates with positive power (pumping) during two load valley periods: noon (11:00–14:00) and night (23:00–05:00), absorbing the surplus photovoltaic and wind power in the system; while it operates with negative power during the morning (08:00–11:00) and evening (18:00–21:00) load peak periods, releasing the stored hydropower energy. Fig. 13 further reveals the dynamic changes of water volume: the water pumping volume curve fluctuates inversely with the water consumption, the water pumping volume rises rapidly during the pumping period, and the water consumption increases synchronously during the power generation period. The water storage capacity of the upper reservoir presents an alternating "double peaks and double valleys" pattern—it first experiences a low valley, then rises to the first peak with pumping, then drops to a deep valley due to power generation during the morning peak, rises rapidly again to the second sharp peak in the afternoon due to noon pumping, and finally falls during the evening peak power generation; the water storage capacity of the lower reservoir is completely opposite, with its peak corresponding to the low valley of the upper reservoir and its deep valley corresponding to the peak of the upper reservoir. Throughout the day, the pumped storage completes two full "pumping-power generation" cycles, effectively converting low-value curtailment of renewable energy into high-value peak-hour electricity, while alleviating the system peak shaving pressure, which reflects the flexible regulation and energy time-shifting capabilities of pumped storage as a large-scale energy storage facility.

In summary, in the new power system with a high proportion of renewable energy, various flexible resources perform their respective duties and complement each other: thermal power units with flexibility modification can track load fluctuations in real time; Price-Based Demand Response (PBDR) helps to flatten the net load curve; Incentive-Based Demand Response (IBDR) can effectively curtail peak loads; both electrochemical energy storage and pumped storage have the dual functions of "peak shaving and valley filling" and promoting renewable energy consumption. The two-stage optimization framework proposed in this paper can fully aggregate and exert the regulation potential of the above-mentioned various resources, significantly improving the overall flexibility and operational reliability of the new power system.

5.3 Comparative Analysis

In order to quantitatively evaluate the marginal contributions of time-based PBDR, segmented IBDR and thermal power flexibility upgrades to the operational performance of the new power system, this study has set up 4 comparison scenarios and conducted a comprehensive comparative analysis from three dimensions: system operation costs, thermal power start-stop characteristics, and backup support capabilities. The details are as follows.

Scenario I: This is the fully resource-coordinated optimization situation proposed in this article. The system simultaneously implements time-based PBDR, segmented IBDR, and flexible retrofit of thermal power generation, and combines electrochemical energy storage and pumped storage to achieve multi-source coordinated dispatch.

Scenario II: Only the segmented IBDR and the retrofitted thermal power generation are retained. The load side does not participate in time-based price-based demand response. This is to evaluate the smoothing effect of PBDR on the net load curve.

Scenario III: The two-stage optimization framework is maintained, but segmented incentive-based demand response is not enabled. It is used for quantitative analysis of the value of IBDR in peak shaving and backup support.

Scenario IV: The thermal power generation units maintain their traditional operating characteristics and do not undergo flexibility retrofit. This is to evaluate the impact of the retrofit on the unit's regulation capability and economy.

5.3.1 Comparison of System Operating Costs

The comparison of the minimum operating costs for each scenario is shown in Fig. 14.

As can be seen from Fig. 14, based on Scenario I, when the time-sharing PBDR is not enabled (Scenario II), the net load curve does not smooth out, and the peak-valley ratio is as high as 1.41. The load fluctuation significantly increases, resulting in an increase of 114,000 CNY in the overall operating cost of the system compared to the benchmark scenario, clearly demonstrating the economic value of PBDR in smoothing the load curve and reducing peak shaving pressure. When the system does not enable segmented IBDR (Scenario III), due to the lack of peak load reduction capability of the incentive-based demand response, the solution cost of the two-stage optimization model is 170,900 CNY higher than the benchmark scenario, reflecting the role of IBDR in alleviating peak load and avoiding the use of expensive peak shaving resources. When the system uses un-flexible-fired power units (Scenario IV), due to the increase in coal consumption rate and the decline in regulation performance of the units, the system operating cost is significantly increased by 422,600 CNY compared to the benchmark scenario, highlighting the key role of flexible power plant transformation in reducing the overall operating cost of the new power system. In summary, the two-stage optimization framework proposed in this paper can fully utilize the regulation potential of demand-side resources, effectively reduce the coal consumption level and carbon emissions of thermal power, and significantly reduce the overall operating cost of the new power system.

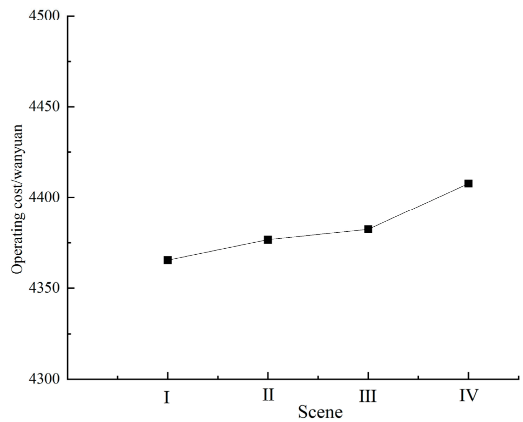

Figure 14: Comparison of operating costs of various scenarios.

5.3.2 Comparison of Startup and Shutdown Characteristics of Thermal Power Units

The data on the start-stop status of thermal power plants, the number of operating units, the number of start-stop operations, and the coal consumption for each scenario are shown in Fig. 8.

From Fig. 8, it can be seen that compared with Scenario I as the benchmark, Scenario II and Scenario III have experienced varying degrees of increases in the number of operating thermal power units, the number of start-stop operations, and the start-stop coal consumption. This is because the PBDR and IBDR fail to actively adjust the load curve, and the system has to rely on the operation and start-stop of more thermal power units to cope with the fluctuating net load, directly resulting in an increase in total coal consumption and more frequent start-stop operations. In Scenario IV, although the number of operating thermal power units and the number of startups are similar to those in the benchmark scenario, the number of shutdowns has significantly increased. The fundamental reason for this is that the units that have not undergone flexibility transformation have limited minimum technical output and climbing rate, and insufficient regulation capacity, unable to effectively follow load changes, causing some units to be forced to shut down, and thus the start-stop coal consumption also increases. In summary, comparing the results of each scenario shows that the synergy between demand response and thermal power plant renovation can effectively reduce the frequency of start-stop operations, reduce start-stop coal consumption, extend equipment lifespan, and improve operational economy.

5.3.3 Comparison of System Backup Support Capability

Since IBDR is a key resource for providing upward adjustment backup, this study focuses on comparing the system backup capabilities of Scenario I and Scenario III, as shown in Fig. 15:

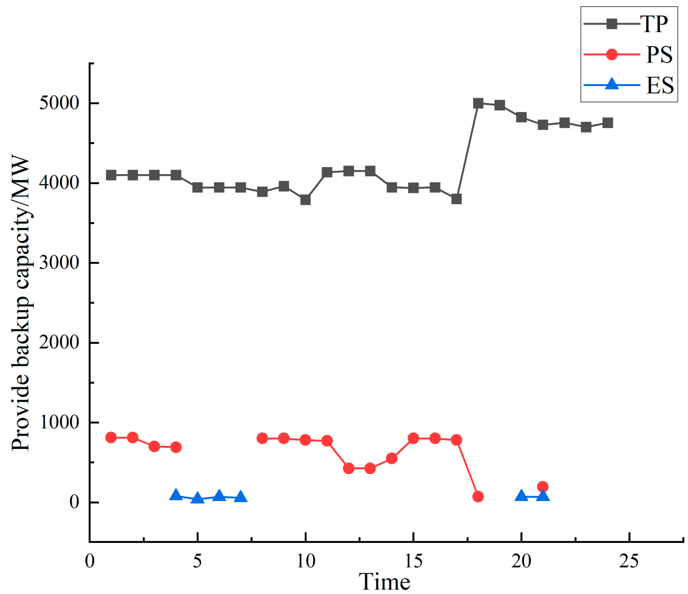

Figure 15: Upper and lower standby capacity provided by various resources in scenario III.

From Fig. 15, it can be seen that in Scenario III without IBDR, the sources of system upward adjustment backup have significantly decreased. Although pumped storage and electrochemical storage can provide some backup, they are limited by capacity and time periods and cannot completely fill the gap after the withdrawal of IBDR. To prevent power supply accidents caused by sudden load increases or sudden drops in the output of new energy, thermal power units have to reserve more upward adjustment backup capacity. This means that a large number of units cannot operate at their efficient rated conditions, miss the opportunity to generate electricity, and directly increase the system's opportunity cost. This comparison clearly proves that IBDR not only can reduce peak loads but also can serve as an important upward adjustment backup resource, effectively sharing the backup pressure of thermal power units, allowing thermal power to operate more stably and economically at the optimal operating point.

6 Conclusions

(1) This paper constructs a two-stage progressive coupling optimal scheduling framework for flexible resource aggregation, which realizes the sequential cooperation of price-based demand response and segmented incentive-based demand response. The first stage effectively smooths the net load curve and reduces the fluctuation variance by nearly half, laying a stable foundation for the second stage of resource scheduling.

(2) The coordinated operation of price-based and incentive-based demand response can not only reduce the peak-valley difference of load and system operation cost, but also provide important upward reserve support for the system, sharing the peak regulation and reserve pressure of thermal power units.

(3) The flexibility transformation of thermal power units greatly improves the operation economy and regulation capacity of the system. Combined with electrochemical energy storage and pumped storage, it realizes the efficient time-space transfer of electric energy, reduces the start-stop frequency and coal consumption of thermal power units, and prolongs the service life of equipment.

(4) The case verification shows that the proposed model has obvious advantages in load fluctuation suppression, operation cost reduction and renewable energy consumption improvement compared

with the traditional scheduling mode, which can provide a reference for the optimal scheduling and flexible resource utilization of high-proportion renewable energy power systems.

Acknowledgement: The completion of this paper has been helped by many scholars. We would like to express our gratitude to them for their help and guidance.

Funding Statement: The work is funded by the Inner Mongolia Autonomous Region Unveilingand Commanding Projects (2022JBGS0044).

Author Contributions: The authors confirm contribution to the paper as follows: Study conception and design: Qiang Li, Yongzhi Liu, Qianpeng Hao, Yaowen Liu, Wenze Li, Zijun Zhao, Zhenyu Chen, Yuxiang Liu, Jiaxing Ren, Wei Han; data collection: Qiang Li, Yongzhi Liu, Qianpeng Hao, Yaowen Liu; analysis and interpretation of results: Wenze Li, Zijun Zhao, Zhenyu Chen, Yuxiang Liu; draft manuscript preparation: Jiaxing Ren, Wei Han. In this research activity, all authors were involved in the data collection and preprocessing phase, model constructing, empirical research, results analysis and discussion, and manuscript preparation. All authors reviewed and approved the final version of the manuscript.

Availability of Data and Materials: The data that support the findings of this study are available from the Corresponding Author, Qianpeng Hao, upon reasonable request.

Ethics Approval: Not applicable.

Conflicts of Interest: The authors declare no conflicts of interest.

Abbreviations

Abbreviation	Full Name
ADN	Active Distribution Network
DER	Distributed Energy Resource
DR	Demand Response
ES	Energy Storage
IBDR	Incentive-Based Demand Response
IES	Integrated Energy System
MILP	Mixed Integer Linear Programming
PBDR	Price-Based Demand Response
PS	Pumped Storage
PV	Photovoltaic
QP	Quadratic Programming
RA	Resource Aggregator
SOS2	Special Ordered Sets of Type 2
TP	Thermal Power
VPP	Virtual Power Plant
WT	Wind Turbine

References

1. Central Committee of the CPC, State Council. Opinions on comprehensively, accurately and fully implementing the new development philosophy and doing a good job in peaking carbon dioxide emissions and achieving carbon neutrality [EB/OL]. [cited 2021 Oct 24]. Available from: http://www.gov.cn/zhengce/2021-10/24/content_5644613.htm.
2. National Development and Reform Commission, National Energy Administration, National Data Administration. Notice on issuing the action plan for accelerating the construction of a new-type power system (2024–2027) [EB/OL]. [cited 2024 Jul 25]. Available from: https://www.gov.cn/zhengce/zhengceku/202408/content_6966863.htm.

3. National Energy Administration. National energy administration releases 2025 national electric power statistics [EB/OL]. [cited 2026 Jan 29]. Available from: https://www.nea.gov.cn/20260129/6874f211acd0417eab7ac10c3061a7c2/c.html. (In Chinese).
4. Gao J, Meng Q, Liu J, Yan Y, Wu H. Multi-energy cooperative optimal scheduling of rural virtual power plant considering flexible dual-response of supply and demand and wind-photovoltaic uncertainty. Energy Convers Manag. 2024;320:118990. [CrossRef].
5. Liang Y, Ji Z, Fan W, Yin Z, Zhao H, Wang Y, et al. Multiple types flexible resources day-ahead and real-time collaborative optimal model adapted to new power system. J Univ Shanghai Sci Technol. 2024;46(4):440–51. [CrossRef].
6. Lu X, Li K, Xu H, Wang F, Zhou Z, Zhang Y. Fundamentals and business model for resource aggregator of demand response in electricity markets. Energy. 2020;204:117885. [CrossRef].
7. Zhong H, Wang D, Peng D, Qu B, Shui J. Optimal scheduling of virtual power plants: An optimization approach combining multi-objective and game theory. Int J Electr Power Energy Syst. 2025;173:111370. [CrossRef].
8. Li X, Cao B, Yang L, Liu C, Li D, Chen K, et al. Aligning adjustable resource flexibility with spot markets using hierarchical model predictive control for park integrated energy systems. Energy Rep. 2026;15:109027. [CrossRef].
9. Zhu H, Ju L, Wang W, Qi X, Nie B, Li X. Multi-agent-based dual-Stackelberg game model and improved benefit allocation strategy for virtual power plant cluster joining in energy and frequency regulation markets. Appl Energy. 2026;413:127682. [CrossRef].
10. Zhao Z, Yu B, Wu Y, Fu J, Dai Y, Wang P, et al. Dynamic energy storage pricing for virtual power plants via bilevel game optimization under multiple uncertainties. J Energy Storage. 2026;154:121259. [CrossRef].
11. Liu X, Huang T, Qiu H, Li Y, Lin X, Shi J. Optimal aggregation of a virtual power plant based on a distribution-level market with the participation of bounded rational agents. Appl Energy. 2024;364:123196. [CrossRef].
12. Jiang XM, Li QF, Yang YW, Zhang LT, Liu XJ, Ning N. Optimization of the operation plan taking into account the flexible resource scheduling of the integrated energy system. Energy Rep. 2022;8:1752–62. [CrossRef].
13. Pan K, Sun T, Pang X, Zheng Z, Li H. Optimal scheduling of integrated energy systems with power-to-hydrogen for flexible supply-demand balance via Q-learning-enhanced grey wolf optimizer. Appl Soft Comput. 2026;192:114795. [CrossRef].
14. Yang H, Yue Y, Gao Y, Liu Y, Zhang D, Shen Y. A two-stage operation reliability evaluation method of distribution system considering dynamic scheduling of flexible resources. Sustain Energy Grids Netw. 2025;44:102011. [CrossRef].
15. Zhong Y, Du Y, Li J, Qian H, Lu F, Jiang Z, et al. Quantitative assessment and optimal scheduling of flexible resources in building district energy systems: A mega-scale real-world case study of 6 million square meters. J Build Eng. 2025;113:114205. [CrossRef].
16. Zhang R, Ni Y, Qiu H, Li Y, Zhang Y, Liu C. Two-stage scheduling model for flexible resources in active distribution networks based on probabilistic risk perception. Energy Eng. 2025;122(2):681–707. [CrossRef].
17. Hu C, Wang H, Li C. Integrated energy system modeling and optimal scheduling strategy for supply and demand side resource flexibility. Renew Energy. 2026;256:124073. [CrossRef].
18. Mirzaei MA, Zare K, Mohammadi-Ivatloo B, Marzband M, Anvari-Moghaddam A. Techno-economic, environmental and risk analysis of coordinated electricity distribution and district heating networks with flexible energy resources. IET Renew Power Gener. 2023;17(12):2935–49. [CrossRef].
19. Zhao T, Cui Z, Wu Z, Duan H, Chen J. Many-objective virtual power plants resource scheduling based on evolutionary multifactorial optimization. Expert Syst Appl. 2026;323:132186. [CrossRef].
20. Li H, Li X, Hao Y, Jin T, Cao Y, Yang Y, et al. Multi-timescale flexible thermal-electric coupling operation of coal-fired thermal power units integrated with molten salt thermal storage system. Energy Eng. 2026;123(4):20. [CrossRef].
21. Moarref B, Abedi SM, Modaresi SM. Optimal scheduling of power system integrated with hydrogen vehicles and flexible resources: A hybrid uncertainty management method. Int J Hydrogen Energy. 2025;100:658–67. [CrossRef].

22. Zhou J, Cai G, Wang Y, Liu C. Dual-timescale scheduling approach for power systems with Energy-intensive loads: Wind power accommodation through forecast deviation decomposition and flexible resource coordination. Energy. 2025;332:136925. [CrossRef].
23. Aliasghari P, Egging-Bratseth R, Stålhane M. Balancing flexibility and longevity: Degradation-aware scheduling of distributed energy resources. Int J Electr Power Energy Syst. 2026;177:111823. [CrossRef].